JACS
JOURNAL OF THE AMERICAN CHEMICAL SOCIETY

Communication

pubs.acs.org/JACS

Cooperative Self-Assembly of Gold Nanoparticles on the Hydrophobic Surface of Vesicles in Water

Ricardo M. Gorgoll,[†] Takuya Tsubota,[†] Koji Harano,*[,†] and Eiichi Nakamura*[,†,‡]

[†]Department of Chemistry, The University of Tokyo, 7-3-1 Hongo, Bunkyo-ku, Tokyo 113-0033, Japan
[‡]CREST, JST, 7-3-1 Hongo, Bunkyo-ku, Tokyo 113-0033, Japan

Supporting Information

ABSTRACT: Adsorption of gold nanoparticles (NPs) on a hydrophobic fullerene bilayer vesicle ca. 30 nm in diameter occurs through cooperation of vesicle/NP and NP/NP interactions to produce a NP−vesicle hybrid whose surface is uniformly covered with the NPs separated from each other by a few nm. The vesicle coverage by NPs makes the NP−vesicle hybrid unusually stable to withstand high temperature, chromatographic purification, and high salt concentration—conditions too harsh for ordinary self-assembled vesicles, such as lipid vesicles, to survive. The hybrid serves as a platform of chemical reactions; for example, gold-catalyzed reduction of an aromatic nitro group and deposition of gold atoms for in situ growth of the NPs from 3.5 to 7.2 nm in diameter. The robust vesicle structure can be destroyed by the heat produced in interparticle plasmon coupling absorption of a 532 nm laser irradiation.

Mesoscopic assemblies of plasmonic nanoparticles (NPs) show collective properties that are produced via coupling of the surface plasmon resonance of neighboring NPs.[1,2] The assembly of NPs on a lipid vesicle, therefore, has been examined as a tool for vesicle functionalization for biological and material applications such as light-triggered release of contents and cell imaging.[3−6] A number of problems have, however, been found as to the stability and control of the density and distribution of NPs on the vesicle, and, most fundamentally, fusion and aggregation of lipid vesicles upon decoration with NPs.[7−10] Here, we report the circumvention of these problems by the use of a bilayer vesicle (**V1**−**V4**) made of a fullerene amphiphile $R_5C_{60}^-K^+$ (**1**−**4**, in the order of decreasing hydrophobicity; Figure 1),[11−13] which is decorated with Au NPs coated with (11-mercaptoundecyl)tetra(ethylene glycol) groups (**NP-1**). These oligo(ethylene glycol) (OEG) chains are capable of binding to the potassium countercation of the anionic vesicle. The decoration of **V1** with **NP-1** (3.5 ± 1.0 nm) took place selectively on one vesicle after another to produce a fully decorated vesicle/NP hybrid (Figure 1a) that undergoes neither aggregation nor fusion. The vesicle, decorated densely with a monolayer of **NP-1** (hereafter hybrid), is stable enough to withstand chromatography purification, and to allow in situ growth of the NPs to 7.2 nm upon treatment with $HAuCl_4$/formaldehyde (Figure 1a). The plasmon effects for the 7.2 nm diameter NP on **V1** were detected spectroscopically and photothermally under laser irradiation. We consider that a vesicle/potassium-bound NP attractive interaction between the negative **V1** surface and the positive **NP-1**/potassium complex (Figure 1b) and the NP/NP attractive interaction operates cooperatively to allow complete NP-coating of **V1**. It is probably this cooperation that is responsible for the stability of the **V1**/**NP-1** hybrid (vide infra).

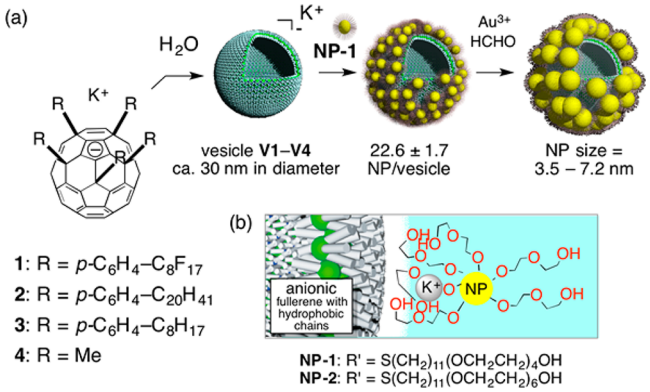

Figure 1. Self-assembly and growth of **NP-1** on fullerene vesicles **V1**−**V4**. (a) Overall scheme. (b) Binding between the **V1** and **NP-1**.

Water-soluble **NP-1**[14−16] (3.5 ± 1.0 nm in diameter of the Au core determined by scanning transmission electron microscopy, STEM. See SI) was synthesized using the Brust method.[17,18] The hydrodynamic diameter determined by dynamic light scattering (DLS) was 8.2 ± 0.1 nm. **NP-1** (concentration of gold atoms = 3.6 mM, 25 °C) shows air−water interface activity,[19,20] as demonstrated by the decrease in the surface tension of a water droplet in air (72.0 mN m^{-1}) to 46.8 mN m^{-1} (Figure 2a and b left, gray line; fitting to the Young−Laplace equation). Fullerene vesicles **V1**−**V4** with an average hydrodynamic diameter of 27−47 nm were prepared in water by spontaneous self-assembly of fullerene amphiphiles **1**−**4**, respectively, as we previously reported.[11,12] We then coated the vesicle surface with the NPs. The vesicles **V1**−**V4** expose hydrophobic alkyl or perfluoroalkyl group at the aqueous interface.

Mixing **V1** (hydrodynamic diameter of 30.4 ± 0.5 nm in pure water) and **NP-1** resulted in spontaneous formation of the hybrid (Figure 1a; Figure 2e−g for images by STEM and scanning electron microscopy, SEM), which is stable enough to be separated from free NPs by Sephacryl (dextran/bis-

Received: April 7, 2015
Published: June 4, 2015

DOI: 10.1021/jacs.5b03632
J. Am. Chem. Soc. 2015, 137, 7568−7571

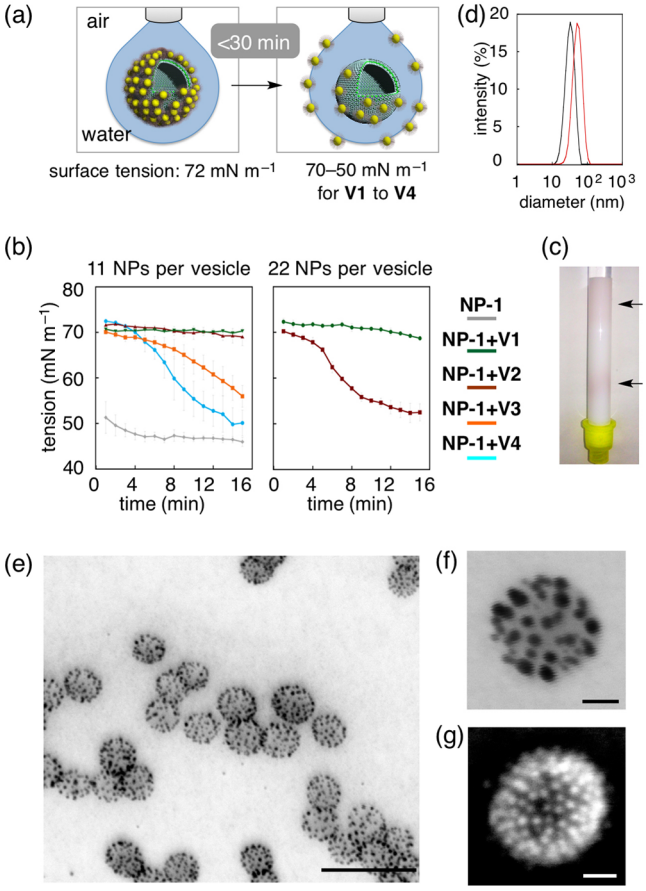

Figure 2. Adsorption of **NP-1** on **V1**–**V4**. (a) Reduction of the air/water surface tension caused by the release of NPs as measured by water droplet pendant method. (b) Time-dependent change of the surface tension of a water droplet in air containing **NP-1**-decorated **V1**–**V4** (cf. Figure 1a). Experiments using a NP/vesicle ratio of 11 are shown on the left graph, and a ratio of 22 on the right. The vesicles have no surface activity under the experimental conditions (<1 mM).[21] Further experimental details are given in the SI. (c) Separation of unbound NPs (top band) from decorated vesicles (bottom band) through a Sephacryl (dextran/bis(acrylamide)) size-exclusion column. (d) DLS size distribution of **V1** before (black line) and after (red line) NP decoration. (e) STEM image of decorated vesicles. The average number of NPs on a vesicle is 22.6 ± 1.7 NP/vesicle. Scale bar is 100 nm. (f, g) STEM and SEM images of a decorated vesicle. Scale bar is 10 nm.

(acrylamide)) size-exclusion chromatography (Figure 2c). The hydrodynamic diameter of **V1** increased from 30.4 ± 0.5 to 49.4 ± 0.2 nm (Figure 2d). The ζ-potential of the vesicles, −45.6 ± 2.4 mV (pH = 7.0), became −13.7 ± 0.8 mV; a value similar to that of **NP-1** (−14.9 ± 3.1 mV). The hydrodynamic diameter of the NP/vesicle hybrid did not change upon heating at 80 °C, providing an additional evidence of this stability. Whereas **V1** immediately precipitates at high salt concentration, the **NP-1**–**V1** hybrid remains stable in phosphate-buffered saline for 8 h at room temperature with ca. 10% increase in the diameter, and the size increase gradually slows down with time (SI). This is probably because NP-decoration converted the ionic vesicle surface into a neutral ethylene glycol-covered surface (Figure 1b). The gold NPs can be recovered from the hybrid by protonation of the vesicle followed by removal of the resulting neutral fullerene by extraction with an organic solvent.

Surface tension measurements of a mixture of **NP-1** and vesicles **V1**–**V4** at the air–water interface indicated particularly strong affinity of **NP-1** to **V1**. Thus, we prepared a droplet from the mixture (time = 0) and measured the time-dependent change of surface tension caused by the movement of **NP-1** from the vesicle surface to the air–water interface (Figure 2a). The surface tension of a reference solution of **NP-1** ([Au] = 0.36 mM) is 46.8 ± 0.4 mN m^{-1}. The first set of experiments was performed for a **NP-1**/vesicle ratio of ca. 11. The surface tension of the solution (70.7–71.6 mN m^{-1}) gradually decreased as **NP-1** moved to the air–water interface (Figure 2b, left). For **V1**, the surface tension decreased slightly after 15 min to 70.3 ± 0.3 mN m^{-1} and 69.0 ± 1.9 for **V2** and significantly to 58.6 ± 0.3 for **V3** and 50.1 ± 2.8 for **V4**, indicating the binding of **NP-1** to **V1**–**V4** decreases as the hydrophobicity of the vesicle surface decreases. Further experiments for **V1** and **V2** with a ratio of 22 indicated that **NP-1** hardly dissociates once adsorbed on **V1** (Figure 2b, right). Thus, we conclude that one of the driving forces for **NP-1** binding to **V1** is the hydrophobicity of the OEG chains when complexed with potassium cation (cf. ability of crown ether to bind on a potassium cation in a hydrophobic solvent).[10,22] The stability of the hybrid at the high salt concentration (vide supra) supports the mechanism. Therefore, we focused on this combination.

The **NP-1**–**V1** hybrid is stable even under electron irradiation in vacuum under the STEM conditions (Figure 2e–g). The STEM vesicle size increased from 30.8 ± 5.2 to 37.7 ± 4.0 nm. The difference of 6.9 nm is twice the size of the gold core of **NP-1**. All vesicles are fully covered with **NP-1** with high uniformity of distribution on the surface (STEM, Figure 2e). The NPs are separated from each other by ca. 2 nm (Figure 2f), which is much shorter than the stretched OEG side chain (2.9 nm) and suggests that in each vesicle, OEG chains interact with each other in the void between the Au cores.[2,23,24]

Experiments using a deficient amount of **NP-1** provided evidence for the cooperation of the two forces in the vesicle/**NP-1** hybrid formation: the vesicle/potassium-bound NP electrostatic attraction (Figure 1b) and the potassium-bound NP/NP hydrophobic interaction. Here, we found that most of the vesicles are either fully or lightly coated by NPs (STEM, Figure 3a and I and II). This observation is quantified for the correlation shown in Figure 3b blue bars (for [Au]/[**1**] = 2.25; i.e., deficiency of NPs), which indicates that the vesicles are either lightly coated ($0 < n < 7$) or densely coated ($13 < n < 33$; note that the number n is related to the diameter of the vesicle). Figure 3b (red bars) provides an additional illustration that a large number of NPs are located on densely decorated vesicles.

The number of vesicles bearing NPs decreases for n = 1–7 and then increases above n = 13–ca. 25 (blue). In Figure 3c (blue dots) we see a linear correlation between the number of NP-coated vesicles and the [Au]/[**1**] ratio, while in Figure 3c (red dots) we see that the average number of **NP-1** on each vesicle is nearly independent of the [Au]/[**1**] ratio. These data agree with a cooperative assembly mechanism initiated by reversible formation of small nuclei followed by rapid irreversible growth of assemblies[25] on the two-dimensional surface of the vesicle.[26]

Interestingly, the mechanism of assembly of Au NPs on **V1** depends on the structure of the OEG side chain. When we used a NP coated with longer chains, (11-mercaptoundecyl)hexa(ethylene glycol) (**NP-2**, 3.2 ± 1.5 nm in diameter of the Au core by STEM and hydrodynamic diameter of 13.2 ± 0.1 nm

DOI: 10.1021/jacs.5b03632
J. Am. Chem. Soc. 2015, 137, 7568–7571

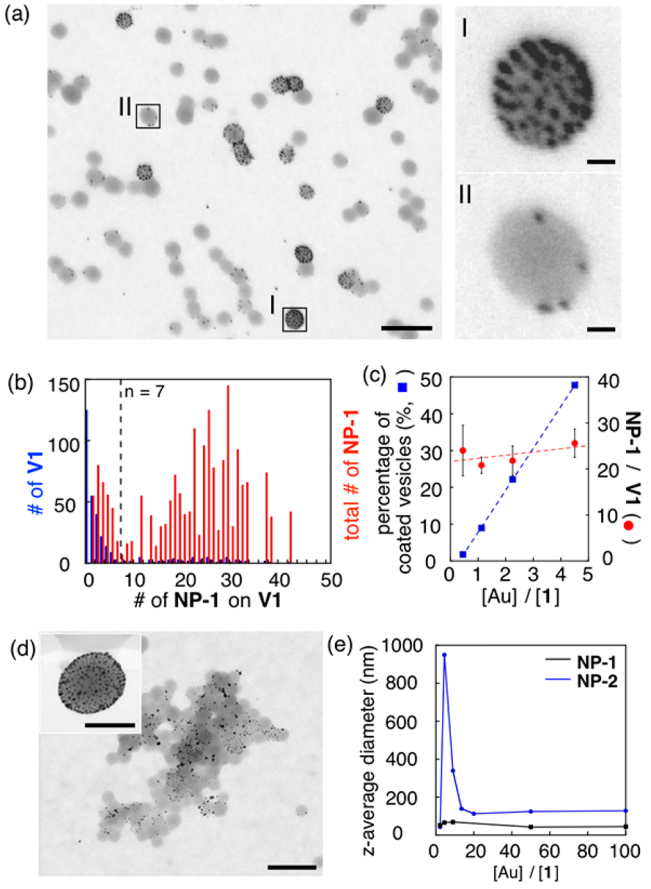

Figure 3. Adsorption of **NP-1** and **NP-2** on vesicle **V1**. (a) STEM image of cooperative adsorption of **NP-1** on **V1**. Scale bar is 100 nm. (b) The number of vesicles bearing an *n* number of **NP-1**/**V1** examined for 339 vesicles. The blue bars indicate the number of vesicles (*x*-axis) bearing *y*-number of NPs on a vesicle. The red bars indicate the total number of NPs on vesicles having *y*-number of NPs. (c) The ratio of NP-1 vs V1 (shown in [Au] and [1] employed for the experiments). The red bars indicate the total number of NPs on vesicles having *y*-number of NPs. (d) STEM image of isodesmic decoration of **NP-2** on **V1** that results in vesicle agglomeration and fusion. Inset shows a large vesicle because of fusion. Scale bars are 100 nm. (e) The [Au]/[**1**] ratio affecting hydrodynamic diameter of assemblies of the hybrid for **NP-1** and **NP-2**. Determined by DLS at 25 °C.

by DLS), the adsorption process became isodesmic probably because of the decreased hydrophobic interaction among potassium-bound **NP-2** (i.e., larger water solubility of **NP-2** than **NP-1**), and the NP-decoration became controlled largely by the vesicle-NP interaction (Figure 1b). Partial decoration of **V1** with NPs resulted in neutralization of the negative charge of the vesicle surface (increased ζ-potential) and hence promoted vesicle agglomeration and fusion, as seen in Figure 3d and inset, respectively.[27] The DLS data in Figure 3e also illustrate the huge difference of the distribution of the size of vesicle/NP hybrids between the **NP-1** and **NP-2** hybrids. A similar phenomenon has been reported for lipid vesicles, where NP causes deformation of the bilayer membrane and vesicle fusion caused by charge neutralization.[8]

NP-1 on **V1** serves as a platform for chemical reactions. **NP-1**–**V1** hybrid (ca. 11 NPs/vesicle) shows a catalytic activity in the $NaBH_4$ reduction of 4-nitrophenol (SI), while neither **NP-1** in water without vesicle nor **V1** show any catalytic activity, indicating the presence of a small area of ligand-free surface on **NP-1**.[28] Another example is the in situ deposition of gold atoms on the adsorbed **NP-1** without destruction of the vesicle structure (Figure 4a–c). Thus, the diameter of **NP-1** was

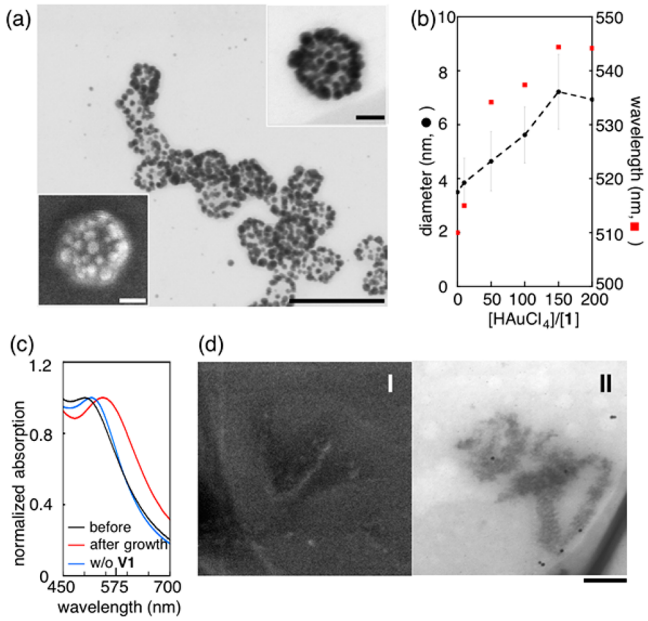

Figure 4. In situ growth of Au NPs on the surface of **V1** and light-triggered collapse. (a) STEM and SEM images of the hybrid after growth of Au NPs ([$HAuCl_4$]/[**1**] = 150). Scale bar is 100 nm. Insets show magnified STEM (top) and SEM (bottom) images of the hybrid (scale bar 10 nm). (b) The ratio of $HAuCl_4$ vs **V1** (shown in [**1**] used) affecting the diameter of the Au NP and the absorption peak wavelength of the surface plasmon resonance. (c) Absorption spectra of free NPs and NPs before and after destruction of the vesicle structure. (d) SEM (I) and STEM images (II) of collapsed vesicles after laser irradiation of **V1** bearing 7.2 nm NPs for 30 min. Loss of the NP and vesicle images is seen. Scale bar is 100 nm.

increased from 3.5 ± 1.0 to 7.2 ± 1.4 nm by adding a solution of $HAuCl_4/K_2CO_3$ (1:3) and formaldehyde (excess) to a solution of **NP-1** on **V1** (2 h at room temperature). By changing the amount of the added gold source ([$HAuCl_4$]/[**1**] in Figure 4b), we noted that the growth stops at 7.2 ± 1.4 nm (black circles), probably because further growth disturbs the OEG network or the growth of a ligand-free surface on the Au NP counterbalances the NP growth. Note that attempts failed to directly decorate **V1** with large Au NPs (6.7 nm in diameter). The observed contact inhibition makes an interesting contrast to the growth of bare Au NPs under the same conditions to a size of 40–50 nm on a polymer-coated carbon nanotube substrate.[29]

The diameter increase accompanied a shift in the NP absorption from 510 to 544 nm (Figure 4b, red squares), which started when the NP grew larger than 4.6 ± 1.1 nm, suggesting the occurrence of plasmonic resonance coupling at this size. The absorption spectra of the **NP-1**–**V1** hybrid before and after growth are shown in Figure 4c and compared with the spectrum of **NP-1** collected after protonative destruction of **V1** (517 nm, as expected for a 7 nm Au NP).[30] Laser irradiation (532 nm, 20 mW, 30 min) of the postgrown NPs of 7.2 nm diameter[31] caused heating by plasmonic effects[32] and destroyed both the NPs and the vesicle (formation of a featureless object in Figure 4d). Laser irradiation of the hybrid bearing the low-

DOI: 10.1021/jacs.5b03632
J. Am. Chem. Soc. 2015, 137, 7568–7571

melting point 3.4 nm NPs resulted in the loss of the NP images and the formation of large Au particles, suggesting that the NPs melted away.

In conclusion, we have decorated a hydrophobic vesicle **V1** through interfacial adsorption of OEG-coated gold NPs in water. By selecting **NP-1** instead of **NP-2** that has longer OEG chains, we decorated one vesicle after another with the NPs because of cooperation of two binding forces, electrostatic attraction between the anionic vesicle and the cationic NP/potassium complex, and hydrophobic interaction among potassium-bound NPs. Here a standard two-step mechanism of nucleation/growth mechanism is expected to occur.[33] On the other hand, **NP-2** randomly decorates many vesicles, partially neutralizes the negative charge of the vesicle, and causes vesicle agglomeration and fusion. The data on **NP-1** thus represent a rare case of cooperative assembly on a spherical surface.[26] The fullerene vesicle is robust enough to allow size-controlled metal atom deposition, suggesting applications for the preparation of multimetallic core−shell structures.

■ ASSOCIATED CONTENT

Supporting Information

Experimental procedures, methods, additional electron microscopy images, and absorption spectra. The Supporting Information is available free of charge on the ACS Publications website at DOI: 10.1021/jacs.5b03632.

■ AUTHOR INFORMATION

Corresponding Authors

*harano@chem.s.u-tokyo.ac.jp
*nakamura@chem.s.u-tokyo.ac.jp

Notes

The authors declare no competing financial interest.

■ ACKNOWLEDGMENTS

This research is supported by KAKENHI (no. 15H05754 to E.N. and no. 26708016 to K.H.), MEXT, Japan. R.M.G. thanks JSPS for a predoctoral fellowship.

■ REFERENCES

(1) Song, J.; Zhou, J.; Duan, H. *J. Am. Chem. Soc.* **2012**, *134*, 13458−13469.
(2) Niikura, K.; Iyo, N.; Higushi, T.; Nishio, T.; Jinnai, H.; Fujitani, N.; Ijiro, K. *J. Am. Chem. Soc.* **2012**, *134*, 7632−7635.
(3) Skirtach, A. G.; Dejugnat, C.; Braun, D.; Susha, A. S.; Rogach, A. L.; Parak, W. J.; Möhwald, H.; Sukhorukov, G. B. *Nano Lett.* **2005**, *5*, 1371−1377.
(4) Jain, P. K.; Huang, X.; El-Sayed, I. H.; El-Sayed, M. A. *Acc. Chem. Res.* **2008**, *41*, 1578−1586.
(5) Wu, G.; Mikhailovsky, A.; Khant, H. A.; Fu, C.; Chiu, W.; Zasadzinski, J. A. *J. Am. Chem. Soc.* **2008**, *130*, 8175−8177.
(6) Mart, R. J.; Liem, K. P.; Webb, S. J. *Pharm. Res.* **2009**, *26*, 1701−1710.
(7) Volodkin, D. V.; Skirtach, A. G.; Möhwald, H. *Angew. Chem., Int. Ed.* **2009**, *48*, 1807−1809.
(8) Michel, R.; Gradzielski, M. *Int. J. Mol. Sci.* **2012**, *13*, 11610−11642.
(9) Zhang, L.; Granick, S. *Nano Lett.* **2006**, *6*, 694−698.
(10) Van Lehn, R. C.; Ricci, M.; Silva, P. H. J.; Andreozzi, P.; Reguera, J.; Voïtchovsky, K.; Stellacci, F.; Alexander-Katz, A. *Nat. Commun.* **2014**, *5*, 4482.
(11) Homma, T.; Harano, K.; Isobe, H.; Nakamura, E. *Angew. Chem., Int. Ed.* **2010**, *49*, 1665.
(12) Homma, T.; Harano, K.; Isobe, H.; Nakamura, E. *J. Am. Chem. Soc.* **2011**, *133*, 6364−6370.
(13) Burger, C.; Hao, J.; Ying, Q.; Isobe, H.; Sawamura, M.; Nakamura, E.; Chu, B. *J. Colloid Interface Sci.* **2004**, *275*, 632−641.
(14) Glogowski, E.; Tangirala, R.; He, J.; Russel, T. P.; Emrick, T. *Nano Lett.* **2007**, *7*, 389−393.
(15) Simpson, C. A.; Huffman, B. J.; Gerdon, A. R.; Cliffel, D. E. *Chem. Res. Toxicol.* **2010**, *23*, 1608−1616.
(16) Alkilany, A. M.; Murphy, C. J. *J. Nanopart. Res.* **2010**, *12*, 2131−2333.
(17) Brust, M.; Bethell, D.; Schiffrin, D. J.; Kiely, C. J. *Adv. Mater.* **1995**, *7*, 795−797.
(18) Kanaras, A. G.; Kamounah, F. S.; Schaumburg, K.; Kiely, C. J.; Brust, M. *Chem. Commun.* **2002**, 2294−2295.
(19) Isa, L.; Calzolari, D. C. E.; Pontoni, D.; Gillich, T.; Nelson, A.; Zirbs, R.; Sánchez-Ferrer, A.; Mezzenga, R.; Reimhult, E. *Soft Matter* **2013**, *9*, 3789−3797.
(20) Binder, W. H. *Angew. Chem., Int. Ed.* **2005**, *44*, 5172−5175.
(21) Harano, K.; Yamada, J.; Mizuno, S.; Nakamura, E. *Chem.−Asian J.* **2015**, *10*, 172−176.
(22) Tracy, J. B.; Kalyuzhny, G.; Crowe, M. C.; Balasubramanian, R.; Choi, J.-P.; Murray, R. W. *J. Am. Chem. Soc.* **2007**, *129*, 6706−6707.
(23) DeVries, G. A.; Brunnbauer, M.; Hu, Y.; Jackson, A. M.; Long, B.; Neltner, B. T.; Uzun, O.; Wunsch, B. H.; Stellacci, F. *Science* **2007**, *315*, 358−361.
(24) Zheng, Y.; Lalander, C. H.; Bach, U. *Chem. Commun.* **2010**, *46*, 7963−7965.
(25) Harano, K.; Homma, T.; Niimi, Y.; Koshino, M.; Suenaga, K.; Leibler, L.; Nakamura, E. *Nat. Mater.* **2012**, *11*, 877−881.
(26) Zhang, K.-Q.; Liu, X. Y. *Nature* **2004**, *429*, 739−743.
(27) Harano, K.; Narita, A.; Nakamura, E. *Chem. Lett.* **2014**, *43*, 877−879.
(28) (a) Biswas, M.; Dinda, E.; Rashid, Md. H.; Mandal, T. K. *J. Colloid Interface Sci.* **2012**, *368*, 77−85. (b) Lee, H.-Y.; Shin, S. H. R.; Abezgauz, L. L.; Lewis, S. A.; Chirsan, A. M.; Danino, D. D.; Bishop, K. J. M. *J. Am. Chem. Soc.* **2013**, *135*, 5950−5953.
(29) Wang, X.; Wang, C.; Cheng, L.; Lee, S.-T.; Liu, Z. *J. Am. Chem. Soc.* **2012**, *134*, 7414−7422.
(30) Nguyen, N. D.; Dang, V. P.; Le, A. Q.; Nguyen, Q. H. *Adv. Nat. Sci.* **2014**, *5*, 045002.
(31) Castro, T.; Reifenberger, R.; Choi, E.; Andres, R. P. *Phys. Rev. B* **1990**, *13*, 8548−8556.
(32) Govorov, A. O.; Richardson, H. H. *Nano Today* **2007**, *2*, 30−38.
(33) Vekilov, P. G. *Nat. Mater.* **2012**, *11*, 838−840.

DOI: 10.1021/jacs.5b03632
J. Am. Chem. Soc. 2015, 137, 7568−7571